

Deep-Red-Emitting Electrochemical Cells Based on Heteroleptic Bis-chelated Ruthenium(II) Complexes

Henk J. Bolink,* Eugenio Coronado, Rubén D. Costa, Pablo Gaviña, Enrique Ortí, and Sergio Tatay

Instituto de Ciencia Molecular, Universidad de Valencia, P.O. Box 22085, ES-46071 Valencia, Spain

Received December 23, 2008

Two ruthenium(II)-based complexes were prepared that show intense deep-red light emission at room temperature. Solid-state electroluminescent devices were prepared using one of the ruthenium complexes as the only active component. These devices emit deep-red light at low voltages and exhibit extraordinary stabilities, demonstrating their potential for low-cost deep-red light sources.

Solid-state light-emitting electrochemical cells (LECs) have attracted considerable interest in the past few years.^{1,2} LECs are single-component electroluminescent devices basically consisting of a film of a charged luminescent material deposited between two electrodes.^{1,3} In its simplest form, LECs are made up of a single active layer composed of an ionic transition-metal complex (iTMC).^{2,4,5} The presence of mobile counterions facilitates the formation of ionic junctions that lower the barrier for electron and hole injection and makes LECs independent of the work function of the electrode material.^{6,7} These characteristics make them suitable for low-cost lighting and signing applications.⁸ The compounds most widely used in these single-component devices are cationic ruthenium(II) and iridium(III) complexes.² Recently, a breakthrough in the stability of LECs was reported by the use of an Ir-iTMC that forms a supramolecular cage via an intramolecular π - π stacking.^{9,10}

* To whom correspondence should be addressed. E-mail: henk.bolink@uv.es.

- (1) Slinker, J.; Bernards, D.; Houston, P. L.; Abruña, H. D.; Bernhard, S.; Malliaras, G. G. *Chem. Commun.* **2003**, 2392.
- (2) Slinker, J. D.; Rivnay, J.; Moskowitz, J. S.; Parker, J. B.; Bernhard, S.; Abruña, H. D.; Malliaras, G. G. *J. Mater. Chem.* **2007**, *17*, 2976.
- (3) Pei, Q.; Yu, G.; Zhang, C.; Yang, Y.; Heeger, A. J. *Science* **1995**, *269*, 1086.
- (4) Lyons, C. H.; Abbas, E. D.; Lee, J. K.; Rubner, M. F. *J. Am. Chem. Soc.* **1998**, *120*, 12100.
- (5) Gao, F. G.; Bard, A. J. *J. Am. Chem. Soc.* **2000**, *122*, 7426.
- (6) deMello, J. C.; Tessler, N.; Graham, S. C.; Friend, R. H. *Phys. Rev. B* **1998**, *57*, 12951.
- (7) Slinker, J. D.; DeFranco, J. A.; Jaquith, M. J.; Silveira, W. R.; Zhong, Y.; Moran-Mirabal, J. M.; Graighead, H. G.; Abruña, H. D.; Marohn, J. A.; Malliaras, G. G. *Nat. Mater.* **2007**, *6*, 894.
- (8) Plummer, E. A.; van Dijken, A.; Hofstraat, J. W.; De Cola, L.; Brunner, K. *Adv. Funct. Mater.* **2005**, *15*, 281.

A wide range of emission colors, including white,¹¹ and efficiencies as high as 36 lm W⁻¹ have been reached.^{12,13} However, only a few examples of deep-red-emitting LECs are reported.¹⁴ Deep-red-emitting LECs are of interest because they can be used in low-cost sensing applications.^{15,16}

The first examples of iTMC-based LECs used ruthenium(II) complexes as the active components. Examples are [Ru(bpy)₃][PF₆]₂, [Ru(dpp)₃][PF₆]₂, and [Ru(tpy)(tpy-CO₂Et)][PF₆]₂, where bpy is 2,2'-bipyridine, dpp is 4,7-diphenyl-1,10-phenanthroline, and tpy is 2,2':6',2''-terpyridine.^{2,14,17–19}

The archetype bis-chelated ruthenium complex is the bis-terpyridine [Ru(tpy)₂]²⁺ cation, which has a very short-living excited state and, consequently, a very low luminance efficiency such that room-temperature emission is not observed.²⁰ Recently, two strategies to obtain bis-chelated ruthenium complexes emitting at room temperature have been reported. The first relies on substitution of the terpyridine with electron-withdrawing or -donating entities on the 4' positions para to

- (9) Bolink, H. J.; Coronado, E.; Costa, R. D.; Ortí, E.; Sessolo, M.; Graber, S.; Doyle, K.; Neuburger, M.; Housecroft, C. E.; Constable, E. C. *Adv. Mater.* **2008**, *20*, 3910.
- (10) Graber, S.; Doyle, K.; Neuburger, M.; Housecroft, C. E.; Constable, E. C.; Costa, R. D.; Ortí, E.; Repetto, D.; Bolink, H. J. *J. Am. Chem. Soc.* **2008**, *130*, 14944.
- (11) Su, H. C.; Chen, H. F.; Fang, F. C.; Liu, C. C.; Wu, C. C.; Wong, K. T.; Liu, Y. H.; Peng, S. M. *J. Am. Chem. Soc.* **2008**, *130*, 3413.
- (12) Tamayo, A. B.; Garon, S.; Sajoto, T.; Djurovich, P. I.; Tsyba, I. M.; Bau, R.; Thompson, M. E. *Inorg. Chem.* **2005**, *44*, 8723.
- (13) Su, H. C.; Wu, C. C.; Fang, F. C.; Wong, K. T. *Appl. Phys. Lett.* **2006**, *89*, 261118.
- (14) Bolink, H. J.; Cappelli, L.; Coronado, E.; Gaviña, P. *Inorg. Chem.* **2005**, *44*, 5966.
- (15) Williams, E. L.; Li, J.; Jabbour, G. E. *Appl. Phys. Lett.* **2006**, *89*, 083506.
- (16) Borek, C.; Hanson, K.; Djurovich, P. I.; Thompson, M. E.; Aznavour, K.; Bau, R.; Sun, Y.; Forrest, S. R.; Brooks, J.; Michalski, L.; Brown, J. *Angew. Chem., Int. Ed.* **2007**, *46*, 1109.
- (17) Kalyuzhny, G.; Buda, M.; McNeill, J.; Barbara, P.; Bard, A. J. *J. Am. Chem. Soc.* **2003**, *125*, 6272.
- (18) Rudmann, H.; Shimada, S.; Rubner, M. F. *J. Appl. Phys.* **2003**, *94*, 115.
- (19) Bolink, H. J.; Cappelli, L.; Coronado, E.; Graetzel, M.; Nazeeruddin, M. J. *J. Am. Chem. Soc.* **2006**, *128*, 46.
- (20) Sauvage, J. P. C.; Chambron, J. C.; Guillerez, S.; Coudret, C.; Balzani, V.; Barigelletti, F.; De Cola, L.; Flamigni, L. *Chem. Rev.* **1994**, *94*, 993.

Table 1. Electrochemical and Photophysical Properties of Complexes **1** and **2**^a

complex	V_{ox} (V) ^b	V_{red} (V) ^b	emission ^c at 298 K		
			λ (nm)	φ_{sol} ^d	τ (ns) ^e
[Ru(tpy) ₂] ²⁺ f	+1.30	-1.24 -1.49	629	$\leq 5 \times 10^{-6}$	0.25
1	+1.41	-0.77 -1.38	723	5×10^{-5}	12
2	+1.46	-0.76 -1.19	717	5×10^{-5}	15

^a Data for the [Ru(tpy)₂]²⁺ complex are included for comparison. ^b vs Fc/Fc⁺. ^c $\lambda_{\text{exc}} = 350$ nm. ^d Deaerated CH₃CN solution (10⁻⁴ M). ^e Luminance emission lifetime $\pm 10\%$. ^f Data from ref 25.

the nitrogen atoms.^{21–23} The second makes use of new tridentate ligands such as aryl-substituted 2-phenyl-4,6-dipyridin-2-yl-1,3,5-triazine (trz).²⁴ Both synthetic routes enhanced the excited-state lifetime and the photoluminescence quantum yield (PLQY) of the bis-chelated ruthenium complexes.

In this Communication, we evaluate two examples of bis-chelated ruthenium emitters using the trz ligand, [Ru(tpy)(trz)][PF₆]₂ (**1**) and [Ru(tpy-CO₂Et)(trz)][PF₆]₂ (**2**), as the single active components in LEC devices. Complexes **1** and **2** were synthesized as explained in the Supporting Information.

The electrochemistry of complexes **1** and **2** was studied in acetonitrile containing [*n*-Bu₄N]PF₆ as the supporting electrolyte versus Fc/Fc⁺ as the internal standard. Electrochemical data are summarized in Table 1, along with reported values for [Ru(tpy)₂]²⁺.²⁵ All of the compounds exhibit one one-electron-reversible oxidation process and two one-electron-reversible reduction processes (see Figure S1 in the Supporting Information and ref 25). B3LYP/6-31G** density functional theory (DFT) calculations (see the Supporting Information for computational details) predict that use of the trz ligand results in a significant stabilization of the highest occupied molecular orbital (HOMO), which is located partially on the ruthenium atom and on the triazine environment (see Figure 1a). The oxidation process is therefore assigned to the extraction of one electron from both the metal center and the trz ligand. The lower energies calculated for the HOMO of [Ru(tpy)(trz)]²⁺ (−6.33 eV) and [Ru(tpy-CO₂Et)(trz)]²⁺ (−6.40 eV) compared with that of [Ru(tpy)₂]²⁺ (−6.20 eV) are in good agreement with the higher anodic potentials measured for **1** and **2** (see Table 1). The lowest unoccupied molecular orbital (LUMO) is fully located on the trz ligand for **1** (−3.07 eV) and **2** (−3.10 eV) (Figure 1b) and is calculated 0.5 eV below the LUMO of [Ru(tpy)₂]²⁺ (−2.60 eV). The stabilization of the LUMO explains the shift of ~0.5 V to less negative values measured for the first reduction potential of **1** (−0.77 V) and **2** (−0.76 V) compared with that of [Ru(tpy)₂]²⁺ (−1.24 V). The second

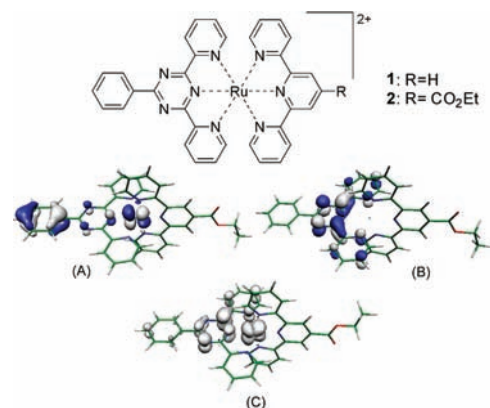


Figure 1. Top: chemical structures of complexes **1** and **2**. Bottom: electronic density contours (0.05 e bohr⁻³) calculated for the HOMO (a) and LUMO (b) of **2** in its ground state S₀; (c) spin-density distribution (0.05 e bohr⁻³) computed for **2** in the lowest-energy triplet excited state T₁.

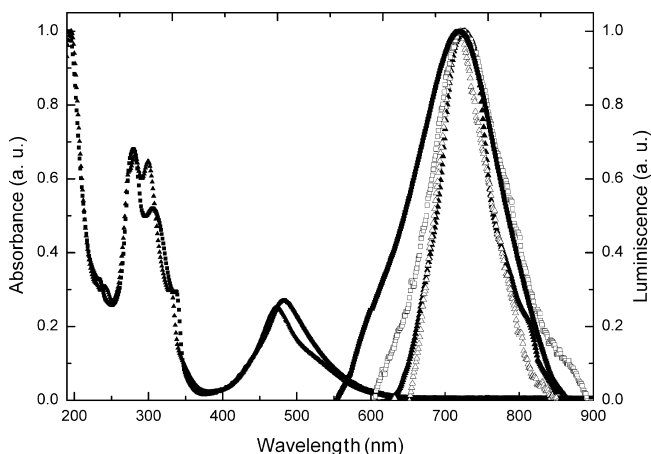


Figure 2. Absorption and photoluminescence spectra in an acetonitrile solution (full symbols) and electroluminescence spectra (open symbols) of complexes **1** (triangles) and **2** (squares). The electroluminescence spectra were obtained from ITO/PEDOT:PSS/complex:PMMA/Al LEC devices using either complex **1** or **2** at an applied bias of 3 V.

reduction process takes place on the tpy ligand and occurs at similar potentials for **1** (−1.38 V) and [Ru(tpy)₂]²⁺ (−1.49 V). It shifts to lower values for **2** (−1.19 V) because of the presence of the electron-attracting ester group.

Figure 2 shows the absorption and photoluminescence spectra recorded for **1** and **2** in a CH₃CN solution. The former exhibit absorption bands typical of ruthenium(II) polypyridine compounds,¹⁴ characterized by ligand-centered $\pi-\pi^*$ transitions in the UV region (190–350 nm) and metal-to-ligand charge-transfer (MLCT) transitions in the visible part of the spectrum (370–620 nm). Moreover, additional bands in the UV region near 300 and 330 nm are ascribed to the lower-energy $\pi-\pi^*$ transitions of the triazine ring.²⁶ In the visible part of the spectrum, two MLCT absorptions are observed for both complexes. The first absorption maximum at ca. 470–490 nm is very similar to that recorded for the [Ru(tpy)₂]²⁺ complex (474 nm)²⁴ and is ascribed to a spin-allowed Ru-to-tpy MLCT transition. In addition, both complexes show a second lower-energy absorption band, which appears as a shoulder at ca. 510–520 nm and is ascribed to a spin-allowed Ru-to-trz MLCT

- (21) Maestri, M.; Armaroli, N.; Balzani, V.; Constable, E. C.; Cargill Thompson, A. M. W. *Inorg. Chem.* **1995**, *34*, 2759.
 (22) Abrahamsson, M.; Wolpher, H.; Johansson, O.; Larsson, J.; Kritikos, M.; Eriksson, L.; Norrby, P.; Bergquist, J.; Sun, L.; Akermark, B.; Hammarstrom, L. *Inorg. Chem.* **2005**, *44*, 3215.
 (23) Medlycott, E. A.; Hanan, G. S. *Chem. Soc. Rev.* **2005**, *34*, 133.
 (24) Polson, M. I. J.; Medlycott, E. A.; Hanan, G. S.; Mikhelsons, L.; Taylor, N. J.; Watanabe, M.; Tanaka, Y.; Loiseau, F.; Passalacqua, R.; Campagna, S. *Chem. Eur. J.* **2004**, *10*, 3640.
 (25) Metcalfe, C.; Spey, S.; Adams, H.; Thomas, J. A. *J. Chem. Soc., Dalton Trans.* **2002**, 4732.

- (26) Nakamoto, K. *J. Phys. Chem.* **1960**, *64*.

transition (Figure 2). The lower energy of these MLCT transitions is due to the low-lying π^* levels of the trz ligand.²⁵

The maximum recorded for the photoluminescence emission of **1** (723 nm) and **2** (717 nm) is red-shifted with respect to the $[\text{Ru}(\text{tpy})_2]^{2+}$ complex (629 nm).²⁵ This shift to lower energies is, in principle, due to the narrower HOMO–LUMO energy gap calculated for $[\text{Ru}(\text{tpy})(\text{trz})]^{2+}$ (3.26 eV) and $[\text{Ru}(\text{tpy}-\text{CO}_2\text{Et})(\text{trz})]^{2+}$ (3.30 eV) compared with that of $[\text{Ru}(\text{tpy})_2]^{2+}$ (3.60 eV). The introduction of the CO_2Et group on the tpy ligand of **2** does not significantly affect the photophysical properties of the complex (see Table 1), in agreement with earlier work by Juris et al.²⁷ It is well-known that the electronic excited state responsible for the luminescence of ruthenium(II) polypyridine complexes is the lowest-lying $^3\text{MLCT}$ state. DFT calculations show that the lowest triplet state (T_1) originates from the HOMO \rightarrow LUMO excitation and is calculated 2.04 eV above the electronic ground state (S_0) in both complexes (adiabatic energy difference). The spin-density distribution computed for the optimized geometry of T_1 is shown in Figure 1c for **2** and has similar values for both complexes (**1**, Ru 0.66e, tpy 0.02e, trz 1.32e; **2**, Ru 0.70e, tpy 0.03e, trz 1.27e). The spin densities confirm the $^3\text{MLCT}$ nature of the emitting T_1 state.

To estimate the phosphorescence emission energy, the vertical energy difference between T_1 and S_0 was computed by performing a single-point calculation of S_0 at the optimized minimum energy geometry of T_1 . Calculations led to vertical emissions of 1.73 eV (717 nm) and 1.71 eV (722 nm) for complexes **1** and **2**, respectively, in good agreement with the observed values (723 and 717 nm, respectively). At room temperature, the solution-based PLQYs of **1** and **2** are 1 order of magnitude higher than that of $[\text{Ru}(\text{tpy})_2]^{2+}$, and the excited-state lifetimes are significantly longer (see Table 1).

Solid films (80 nm) of **1** and **2** blended with 20% by weight of poly(methyl methacrylate) (PMMA) were obtained by spin-coating from acetonitrile solutions. Prior to the deposition of the active layer, a thin layer (100 nm) of poly(ethylene dioxythiophene)–poly(styrenesulfonic acid) (PEDOT:PSS) was spin-coated on top of the indium–tin oxide (ITO)-coated substrates to increase the reproducibility of the devices. An aluminum electrode was evaporated on top of the spin-coated thin films. Device preparation and characterization was performed in an inert atmosphere (<0.1 ppm H_2O and <0.1 ppm O_2). Upon application of a bias of 3 V to an ITO/PEDOT:PSS/complex:PMMA/Al device, light emission and current density, slowly increasing in intensity with time, are observed. The electroluminescence spectra are broad and have shapes similar to those of the photoluminescence spectra obtained from the complexes in solution (Figure 2). They show a maximum around 717 and 725 nm for **1** and **2** devices, respectively. This deep-red light emission is the lowest-energy emission observed so far in LEC devices based on ruthenium complexes.

The temporal behavior of LEC devices using either complex **1** or **2** at an applied bias of 3 V is depicted in Figure 3. The buildup of the light output is synchronous to the current density. Maximum light outputs around $0.6 \mu\text{W}$ are

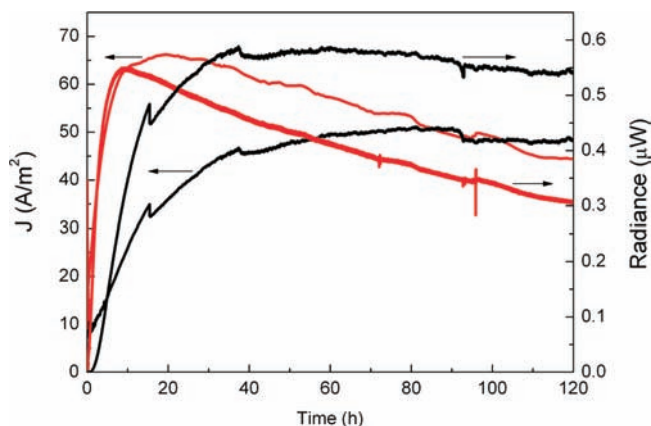


Figure 3. Current density and radiance evolution as a function of time for LEC devices using either complex **1** or **2** (red and black, respectively) at an applied bias of 3 V.

reached after approximately 9 and 37 h for the devices using complexes **1** and **2**, respectively.

Although the CO_2Et group barely affects the electrochemical and photophysical properties, it has a noticeable effect on the device properties. The LEC based on complex **2** has a significantly higher turn-on time, indicative of the lower mobility of the PF_6^- anions. Additionally, the device stability also increases when complex **2** is used. At the maximum light output, the external quantum efficiency reaches values of around 0.005% in both LEC devices. Another striking feature is the long lifetime of the device. Compared with the longest-living ruthenium-based LECs, the device with complex **1** has similar lifetimes (time to reach half of the initial luminance) around 120 h. The device using complex **2** reaches a significantly longer lifetime of at least 360 h. Luminance and current density have a similar dependence versus time, which is an indication that the degradation of the device is caused by a loss of charge injection or transport and is not due to the degradation of the emitting molecules.

In conclusion, two room-temperature light-emitting bis-chelated ruthenium complexes using 2-phenyl-4,6-dipyridin-2-yl-1,3,5-triazine as one of the ligands have been prepared. Solid-state LECs that use these complexes as the main active component emit deep-red light. Surprising device stabilities are observed compared to previously reported device lifetimes, which indicates that the complexes are quite robust toward degradation reactions.

Acknowledgment. This work has been supported by the European Union (Heteromolmat, STRP 516982), ESF Eurocores-05SONS-FP-021, the Spanish Ministry of Science and Innovation (MICINN) (MAT2006-28185-E, MAT2007-61584, CTQ2006-14987-C02-02, and CONSOLIDER-INGENIO CSD2007-00010), the Generalitat Valenciana (Grant GVAINF/2007/051), and European FEDER funds (Grants CTQ2006-14987-C02-02 and GVAINF/2007/051). H.J.B. and R.D.C. acknowledge the support of the Program “Ramon y Cajal” and a FPU grant respectively of the MICINN.

Supporting Information Available: Experimental procedures and analytical and theoretical data. This material is available free of charge via the Internet at <http://pubs.acs.org>.

(27) Juris, A.; Balzani, V.; Barigelli, F.; Campagna, S.; Belser, P.; von Zelewsky, A. *Coord. Chem. Rev.* **1988**, *84*, 85.